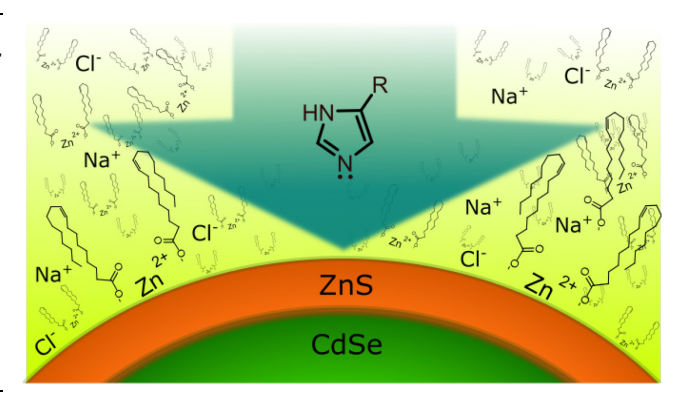
Coordination of Quantum Dots in Polar Solvent by Small-Molecule Imidazole Ligands

Nuwanthaka P. Jayaweera, John H. Dunlap, Fiaz Ahmed, Taylor Larison, Leman Buzoglu Kurnaz, Morgan Stefik, Perry J. Pellechia, Augustus W. Fountain III, and Andrew B. Greytak*

Department of Chemistry and Biochemistry, University of South Carolina, Columbia, South Carolina, USA 29208 KEYWORDS CdSe/ZnS, Core/Shell Quantum Dots, Oleate, Imidazole, Small-molecule Ligands

ABSTRACT: Colloidal quantum dots (QDs) are attractive fluor-ophores for bioimaging and biomedical applications because of their favorable and tunable optoelectronic properties. In this study, the native hydrophobic ligand environment of the ole-ate-capped sphalerite CdSe/ZnS core/shell QDs was quantitatively exchanged with a set of imidazole-bearing small-mole-cule ligands. Inductively coupled plasma-optical emission spectroscopy and 'H-NMR were used to identify and quantify three different ligand exchange processes: Z-type dissociation of the Zn(oleate)₂, L-type association of the imidazole, and X-type anionic exchange of oleate with Cl⁻, all of which contribute to the overall ligand exchange.



INTRODUCTION

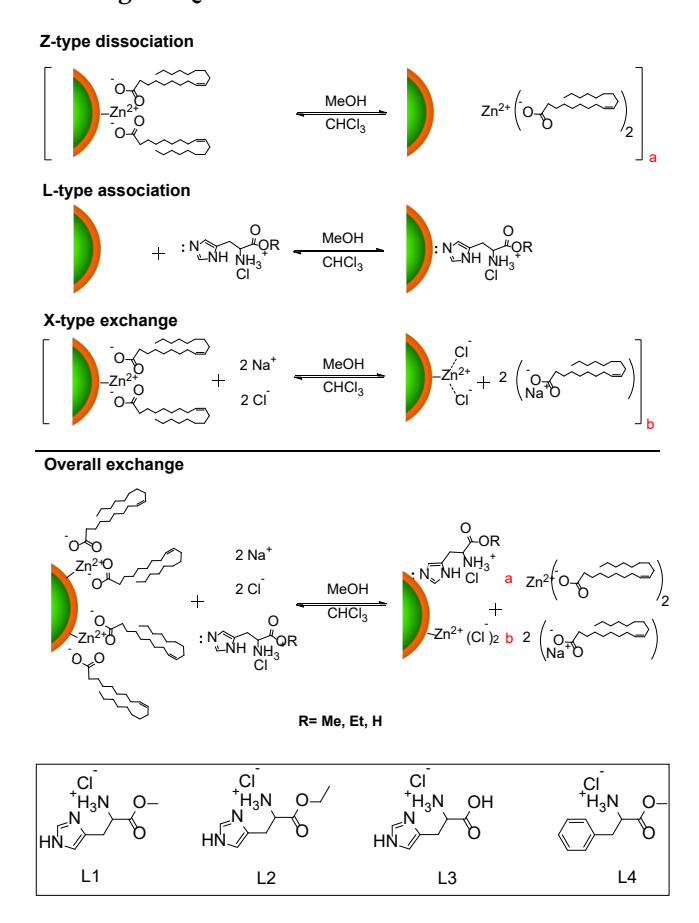
For bioimaging applications of quantum dots,¹⁻¹³ exchange of native hydrophobic ligands with small molecules can achieve water solubility while preserving a small hydrodynamic radius.¹⁴⁻¹⁶ Several types of hydrophilic ligands have been identified for ligand exchange of fluorescent QDs.¹⁷⁻²⁷ Numerous studies on thiol anchoring groups show their high binding strength to the QD surface. However, thiols are not an ideal solution for bioimaging applications. The susceptibility of QD-thiol conjugates to oxidation, photoluminescence (PL) quenching, and nonspecific binding prevent them from being effectively used in biomedicine.^{18,28-32}

Therefore, researchers have turned to imidazoles as the anchoring group of choice for bioimaging applications. Imidazole-bearing copolymers have shown promising results in bringing QDs into polar solvents and maintaining low cytotoxicity and low non-specific binding.^{32–37} The imidazole anchoring group has shown good affinity for the undercoordinated metal sites on the QD surface while maintaining a high quantum yield and being resistant to oxidation.^{32,33} Inspired by early results with polyhistidine-tagged peptides, research has focused on synthetic polymeric imidazole ligands since they appear to show higher binding affinity toward the QD surface compared to small molecules and, therefore, relatively high stability in polar solutions.^{32,33,38-40} However, the main drawback to polymeric

imidazole ligands is their large molecular sizes and random packing at the QD surface, creating a risk of undercoordinated sites on the QD surface.^{33,41} Small-molecule ligands can reach the QD surface efficiently to prepare a well-packed coating, which could both increase the solubility of the QDs in polar environments and also diminish oxidation at the QD surface. However, examples of QDs stabilized by small molecule imidazole coordination are lacking. A study of nucleophilic coordination of CdSe QDs in benzene found that alkylimidazole could displace phosphines but did not lead to colloidal stability even at high ligand concentrations.⁴²

Herein, we describe a small-molecule model for imidazole coordination in a polar solvent that permits systematic investigation. Initially oleate-capped QDs (QD-OA) can undergo three types of ligand exchanges under the experimental conditions (**Scheme 1**): Z-type dissociation of Zn(oleate)₂, L-type nucleophilic association of the imidazole ligands, and X-type anionic exchange of the oleate ligands with Cl⁻. In this study, we report sphalerite (zincblende) CdSe/ZnS core/shell QDs that are coordinated by histidine and two histidine-derived esters (**L1**, **L2**, and **L3**) as small molecule imidazole ligands. Quantitative analytical measurements identified the number of boundoleate ligands per QD, the amount of oleate removed from the QD surface, and the percentages of the Z-type dissociation and X-type exchange.

Scheme 1: Representative reactions comprising ligand exchange of QD-OA with imidazole derivatives



EXPERIMENTAL SECTION

Preparation of CdSe/ZnS and CdSe/CdS core/shell QDs. Sphalerite core/shell CdSe/ZnS and CdSe/CdS QDs with a 1.6 monolayer shell thickness and oleate ligand termination were synthesized using a previously described method for the cores,^{43,44} followed by shell growth using SILAR.⁴⁵⁻⁴⁷ (Additional detail is found in Supporting Information). Before the ligand exchange, oleate-QDs were purified using one cycle of precipitation and redispersion (1xPR), followed by GPC in toluene⁴³ to remove growth solvent and excess oleate ligands.

Ligand exchange procedure. A sample of GPC purified core/shell QDs (10 nmol) was brought into CHCl3 (2mL). L1 (0.0364g) was dissolved in 10mL of methanol and the pH of the mixture was adjusted to 7.0 by adding saturated NaOH in methanol (pH was measured by bringing an aliquot of the methanol mixture in to deionized water). Finally, the volume of the mixture was adjusted to 15 mL to achieve a ligand concentration of 10 mM. The solution of L1 (2 mL) was added to the OD sample dropwise over 30 min while stirring. The homogeneous mixture was allowed to stir for another 30 min before degassing to dryness with N2. Ligand-exchanged QDs were then dispersed in 2 mL of methanol and washed with 3 mL of hexane three times. The hexane layers were separated carefully to remove displaced oleate from the mixture and combined for further analysis. Purified ODs and an aliquot of the hexane layer were characterized by optical and ¹H NMR spectroscopy. Another aliquot of the hexane layer was used for ICP-OES analysis.

Reactions for ligand exchange with L2, L3, and L4 were carried out under the same conditions as described above for L1.

GPC Purification of small-molecule imidazole capped QDs. Excess small-molecule imidazole ligands were removed from the initial ligand exchanged QD sample by a size exclusion chromatographic technique. Here, 10 nmol of the small-molecule imidazole capped QDs were purified by a GPC column with Sephadex LH-20 using methanol as the mobile phase. The purified sample was collected when the elution volume reached about 1/3 of the total volume of the column. The GPC column was rinsed thoroughly (3× total column volume) between successive purifications.

Optical spectroscopy. Formation of QDs, shell growth, and ligand exchange was monitored by UV–visible absorption using a Thermo Scientific Evolution Array spectrophotometer with hexane (before ligand exchange) or methanol (after ligand exchange) as solvents as well as the blank in a 1 cm path quartz cuvette. The fluorescence spectra were also recorded to monitor the growth and size distribution of the QDs. Emission spectra were recorded by an Ocean Optics USB 4000 spectrometer under ~365 nm excitation.

The absolute quantum yield (QY) of the initial and ligand exchanged samples are estimated by quantitative comparison to rhodamine 640 perchlorate (R640, QY = 95% in methanol). Photoluminescence spectra of QD samples and R640 dye were taken under the same spectrometer conditions on a Horiba fluorescence spectrometer in triplicate and averaged. The optical density of the samples was kept below 0.1 between 500 and 700 nm to avoid internal filtering effects, and excitation wavelengths were selected at points of similar optical density. The quantum yield was calculated based on the integrated intensities (area under the curve) of the emission spectra, the absorption at the excitation wavelength, and the index of refraction of the solvent based on established methods.⁴⁸

Inductively Coupled Plasma-Optical Emission Spectroscopy analysis. According to a previously published procedure,49 samples for ICP-OES were prepared by drying an aliquot of the hexane layer (2 mL) in a 15 mL high-density polyethylene narrow mouth bottle sealed by a rubber septum under vacuum to remove all the solvent. A 0.5 mL aliquot of 30% aqueous hydrogen peroxide solution was added to the dried sample, and the polyethylene bottle was quickly and tightly closed. The sample was allowed to digest for 5 min, and then a 0.5 mL aliquot of 70% aqueous nitric acid solution was added, and the bottle was closed again. The reaction mixture was allowed to digest for another 30 minutes. Finally, the samples were diluted by adding 6 mL of DI water (18.3 M Ω -cm). Calibration solutions were prepared using a commercial multielement calibration standard containing 24 elements (Spex CertiPrep CL-CAL-2, Lot Number CL3-12MJY). Final concentrations of the calibration standards were set to o (blank), 0.00625, 0.0125, 0.025 and 5 µg/L, respectively. Emission spectra were collected at the following wavelengths: for Cd, 214.4, 228.8, and 361.0 nm, for Se, 196.0 and 203.9 and 206.2 nm, and Zn 330.2, 334.5, 481.0 nm.

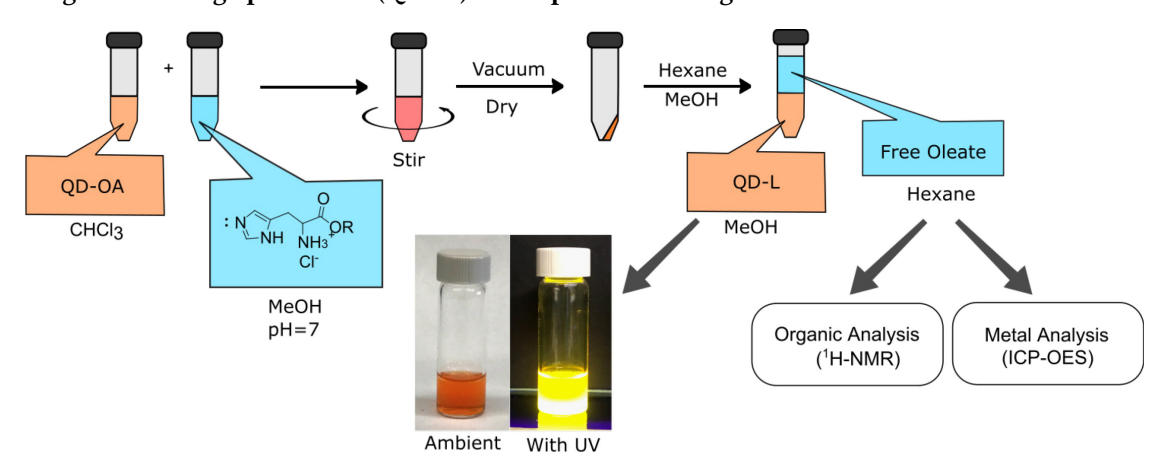
¹H NMR analysis. Samples were prepared by dissolving the initially purified QDs, purified ligand exchanged QDs, and aliquots of the hexane layer in deuterated solvents (CDCl₃ for initial QDs and CD₃OD for ligand exchanged QDs). Initial QD samples were isolated using one cycle of precipitation and redissolution by using acetone and methanol and were brought into CDCl₃. Then, all the samples were dried under vacuum on a Schlenk line. The samples were then dissolved in a known

amount of the respective deuterated solvents and transferred into an NMR tube. Spectra were recorded using a Bruker Avance III HD 400 with 64 scans and a 15 s relaxation delay. The concentration of the oleate/oleic acid in the hexane layer was evaluated using hexamethylcyclotrisiloxane as the internal standard. Variable-temperature analysis was performed using 10 nmol L1-capped QDs or a similar total concentration of neutralized L1 ligand in 1 mL methanol-d4

Zeta potential (ζ) and dynamic light scattering (DLS). For each of these measurements, samples (~5 nmol) of oleate

capped QDs (in CHCl₃), L₁ capped, L₂ capped and L₃ capped QDs (in MeOH) were brought into 2 mL solvent and added into quartz cuvettes. Measurements were performed using a Zetasizer Nanoseries ZEN₃690 instrument. Measurements of ζ using a quartz cell were run 3 times per sample at 25°C to obtain average and standard deviation. Measurement of hydrodynamic diameter (HD) via DLS were collected over 90s for 5 runs, 3 times per sample at 25°C using appropriate plastic cuvettes.

Scheme 2: Ligand exchange procedure (QD-L1) and biphasic washing to remove free oleate



RESULTS AND DISCUSSION

Initially, ligands L1-L4, received as hydrochlorides, were dissolved in methanol, and the solutions were titrated using a saturated NaOH solution in methanol such that aliquots diluted in water indicated a pH of 7.0. Adjusting the pH of the ligand solution showed that the dihydrochlorides and the neutral bases of L1 and L2 were not effective in ligand exchanges. We believe the presence of the positive charge on the ligand backbone allows it to interact with the polar solvents while electrostatic stabilization with bound Cl- on the surface of the QD improves the binding. The final concentrations of the ligands in methanol were set to 10 mM. Ligand exchange was accomplished in a homogeneous mixture of chloroform and methanol, followed by washing of the ligand-exchanged QDs with hexane as outlined in Scheme 2.

Imidazole-bearing ligands successfully underwent the ligand exchanges with CdSe/ZnS QDs, but the treatment of CdSe/CdS QDs under the same conditions was unsuccessful, with addition of ligands promoting aggregation. We note that weaker coordination of Cd²+ than Zn²+ by amine ligands has been reported in molecular complexes.⁵⁰ As expected, L4, which lacks an imidazole ring, was not able to make colloidally stable QDs in methanol, suggesting that the imidazole group is indeed responsible for surface coordination in L1, L2, and L3. In addition, attempted ligand exchange with analogues of L1 in which the amine was acylated to a non-ionic amide were unsuccessful, indicating a role for the primary amine in stabilizing the ligand-exchanged QDs.

Purification of the ligand-exchanged QDs was accomplished in two stages. Firstly, ligand-exchanged QDs dissolved in methanol were washed thrice with hexane to remove the extruded oleate ligands. The hexane fractions were collected and combined for later analysis. The washed QDs were then further purified using GPC to separate the QDs from unbound imidazole ligands (Sephadex LH-20, methanol mobile phase: Supporting Information Figure S5). To confirm the separation of the free L1 ligands from the QD-L1, 1 mL fractions were collected from 4 mL to 16 mL after injection of the QDs onto a column of ~13 mL total bed volume. The majority of the QD-L1 were isolated in the 5 mL and 6 mL fractions. The QDs could be identified by their visible absorption, while ligands were visualized using a ninhydrin probe, making use of the primary amine group in L1-L3. QD-L1 in the fractions 5-6 and free L1 in the fractions 9-11 became dark purple after the ninhydrin test. This was an initial confirmation that the QDs are capped by the L1: the orange color spots for fractions 5-6 changed to dark purple after the ninhydrin test.

UV-Vis and PL maxima did not show a significant shift upon ligand exchange (**Figure 1**). Among the ligands tested, **L1** and **L2** imparted high colloidal stability in methanol over a period of weeks, while QDs exchanged with **L3** displayed increased light scattering and flocculation within 24 h.

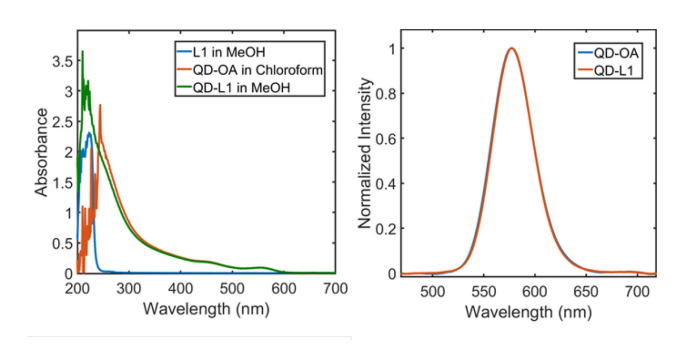


Figure 1. Absorption (left) and emission (right, 365 nm excitation) spectra of CdSe/ZnS QDs before and after ligand exchange with L1.

Fourier-transform infrared (FTIR) spectra of the QDs before and after ligand exchange with L₁, collected in an attenuated total internal reflection (ATR) geometry, are depicted in Figure 2 (additional results in **Supporting Information Figures S6-S8**). The oleate-capped QDs have asymmetric CH₂ vibrations at 2923.5 cm⁻¹, symmetric CH₂

vibrations at 2853.0 cm⁻¹, asymmetric COO⁻ vibrations at 1545.1 cm⁻¹, and symmetric COO⁻ vibrations at 1457.6 cm⁻¹, 5¹ The FTIR spectrum of L1, (red in Figure 3) shows N-H bend out-of-plane vibration at 623.6 cm⁻¹, C-H bend out-of-plane vibrations at 832.6 cm⁻¹, and C-H bend vibrations at 1082.2 cm⁻¹ which are related to the imidazole ring. QD-L1, QD-L2, and QD-L3 all demonstrate a similar pattern to free ligands, but with significant frequency increasement in the imidazole resonances, reflecting the imidazole ring bonds' strengthening by electropositive Zn²⁺ metal ions on the QD surface (Supporting Information Figures S7-S8).⁵² This is conclusive evidence that the incoming ligands bind to the QD surface via imidazole.

The 'H-NMR spectrum of GPC-purified **QD-OA** in toluene (blue in **Figure 3**) has a broad peak at 5.56 ppm, confirming the bound-oleate population, while the 'H-NMR spectrum of **L1** in methanol (red) shows peaks at 6.89 ppm and 7.61 ppm that correspond to the imidazole ring protons. Purified **QD-L1** (green) indicates both imidazole and oleate ligands present in the sample.

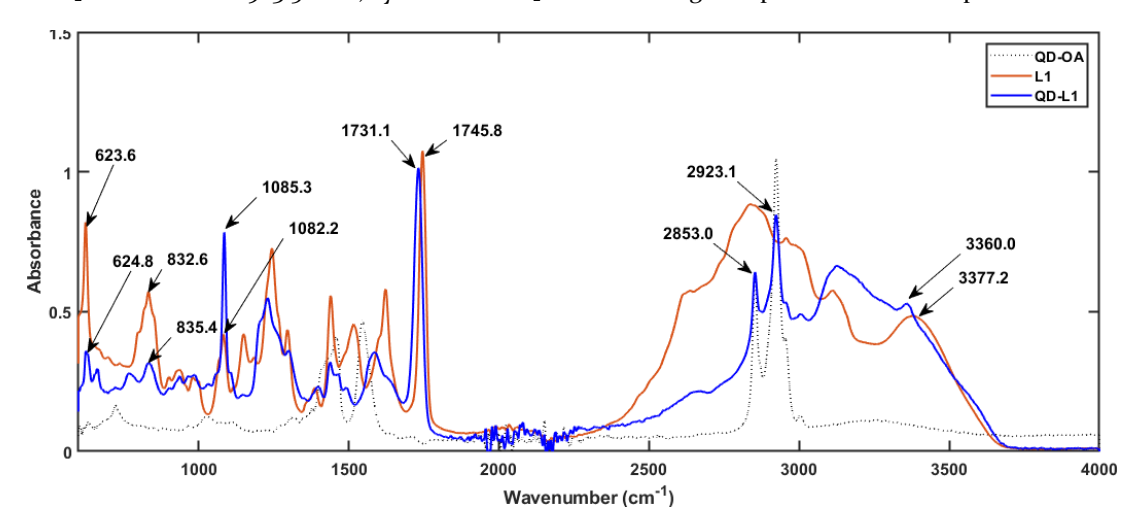


Figure 2. FTIR characterization of ligand exchange with L1.

We used variable temperature ¹H-NMR (VT-NMR) to further investigate the binding of imidazole ligands to the QD surface. Compared to free L1, QD-L1 in the same solvent shows peak broadening at lower temperatures (Figure 4). Even though ligand coordination is clearly evident, it remains dynamic in the sense of rapid exchange with solution-phase and/or other QDs. An apparent consequence is that QD-L1 could not be brought into water or aqueous buffers, despite several attempts and conditions. The contrasting experience with imidazole-bearing polymers, which have been used previously by our group and others to bring similar QDs, including wurtzite CdSe/CdS into water,733344.9640.53-56 suggests that the polymer-capped QDs are indeed thermodynamically stabilized by multiple coordination at the QD surface.

To further characterize the products, we employed a quantitative approach using both inductively coupled plasma optical emission spectroscopy (ICP-OES) and ¹H-

NMR spectroscopy. Initially, the extruded oleate ligands were collected from the ligand exchanged QD samples by combining the three hexane fractions from the washing steps. Then, an aliquot of the extruded sample (hexane layer) was used to find the concentration of metal by ICP-OES. Another aliquot was used to find the concentration of oleate ligands simply by using quantitative 'H-NMR, where hexamethylcyclotrisiloxane was used as the internal standard, to arrive at the relative ligand and metal amounts per QD. Results are summarized in **Table 1**.

According to the quantitative 1 H-NMR, up to 77% of the oleate ligands present in **QD-OA** are removed from the QD surface on formation of **QD-L1** (Supporting Information **Fig. S9-S10**). Analysis of the hexane wash suggests that about 32% of the departed oleate was accompanied by Zn (representing Z-type dissociation of $\text{Zn}(\text{OA})_2$) while the remainder (about 68%) were not accompanied by loss of Zn and are presumed to have undergone X-type exchange

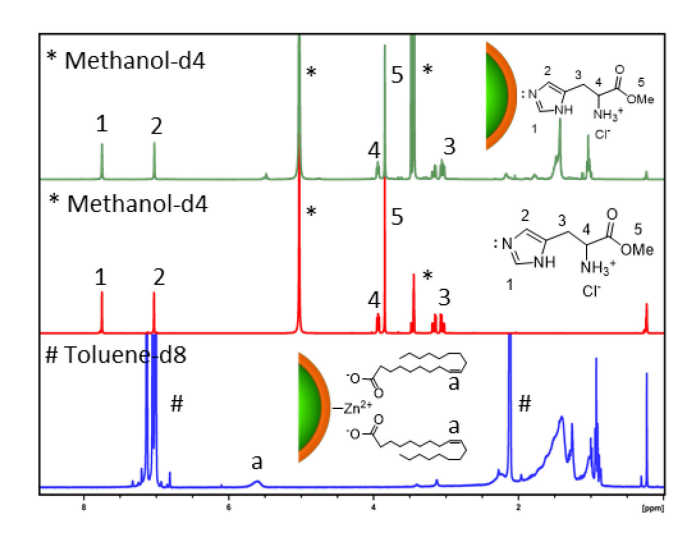


Figure 3. 'H-NMR characterization of ligand exchange with L1. (NMR standard hexamethylcyclotrisiloxane peak resides at 0.2 ppm).

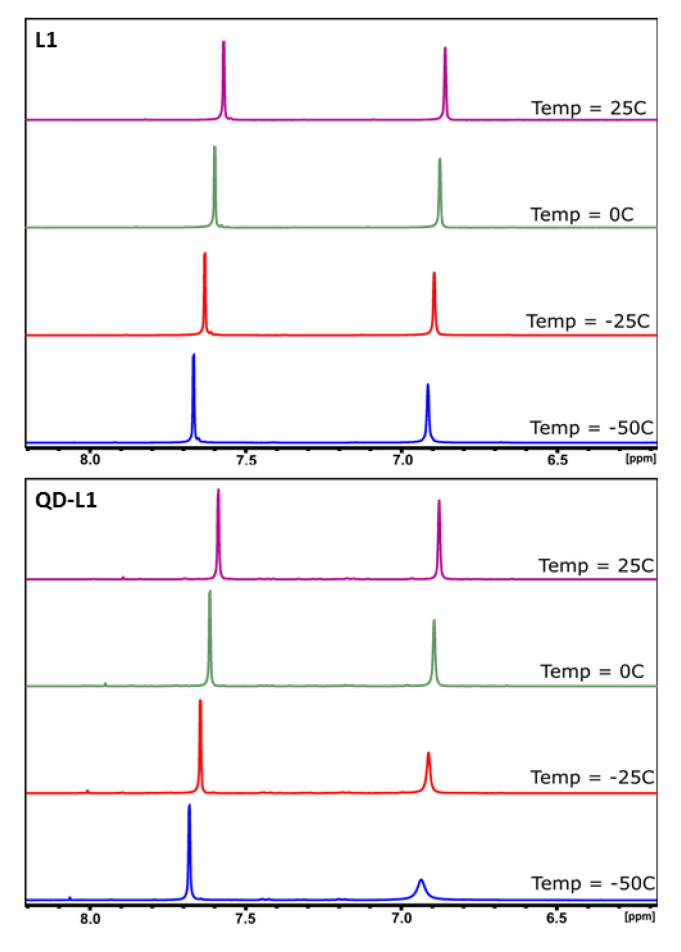


Figure 4. Variable Temperature ¹H-NMR spectra of L1 (top) and QD-L1 (bottom) focusing on imidazole C-H protons.

in which they are replaced by chloride, maintaining approximate charge balance. Dissociation of a substantial fraction of the oleate ligands from the QD surface allows the L-type association of the small-molecule imidazole ligands L1-L3; in fact, it almost doubled the ligand population on the QD surface overall based on ¹H NMR of the QDs in methanol. We note that previous studies of sphalerite-

based CdSe QDs demonstrated that the number of vacant coordination sites on (111) surfaces exceeds the number of monovalent anions required for charge balance and that additional coordination sites can be occupied by neutral amine ligands binding through L-type coordination.⁵⁷ SEM-EDAX analysis of **QD-L1** before and after GPC purification confirms X-type exchange with Cl⁻ since almost all the Na⁺ is removed from the QD sample after the ligand exchange, while a significant amount of Cl⁻ is still present in the purified QD sample. Exchange of oleate with Cl⁻ has also been reported in CdSe, but colloidal stability could not be maintained by coordination of alkylimidazole in that case.^{42,58}

Table 1: Quantitative analysis of the ligand exchange using 'H-NMR and ICP-OES

		QD-OA	QD-L1	Hexane Wash
NMR	OA:QD	118 ± 2	27 ± 2	71±2
	L1:QD	N/A	186 ± 2	0
ICP-OES	Zn:QD			11.6 ± 0.4
	Cd:QD			0.012 ± 0.003
	Se:QD			1.57 ± 0.16

Nearly 60% of the PL quantum-yield (QY) was maintained after the ligand exchange of oleate-capped QDs with L1: Table 2 compares the absolute QY of QD-OA in toluene (following GPC purification) and of imidazole-capped QDs in methanol. Zeta potential measurements suggest that the initial negatively charged environment of the QD surface, terminated with oleate ligands, changes to a positively charged surface when capped with the imidazoles. We attribute the positive ζ potential, which approaches the 25 mV thermal voltage considered a threshold for long-term charge stabilitization, to partial dissociation of primary ammonium chloride functions on L1-L3 in the methanol solvent.

Table 2. Quantum Yield, Zeta Potential, and DLS

QD Type	QY (%)	ζ (mV)	HD (nm)
QD-OA	41.3	-19.9±3.0	4.1 ± 1.3
QD-L1	24.7	20.9 ± 3.9	3.1 ± 0.5
QD-L2	24.2	17.7 ± 0.4	3.8 ± 0.5
QD-L3	17.3	22.6 ± 0.3	6.5 ± 1.0

We note that previous efforts to stabilize chalcogenide QDs in anhydrous solvents with L-type ligands have encountered difficulty; stability appears to rely on steric stabilization from bulky X-type ligands such as oleate. In the present case, protonation of the amine-bearing imidazoles seems to contribute a measure of charge stabilization in methanol. The hydrodynamic diameter (HD) values acquired through dynamic light scattering experiment show QD-L1 and QD-L2 have smaller radii than QD-OA, which

is expected for well-dispersed samples, as the imidazole ligands we have chosen are smaller than the oleates. In contrast, the higher HD of QD-L3 is likely a result of partial aggregation: indeed, we note that QD-L3 had relatively low colloidal stability, displaying visible flocculation and precipitation within 24 hours.

CONCLUSIONS

We have described successful ligand exchanges starting from oleate-capped CdSe/ZnS core/shell QDs with a series of small-molecule imidazole ligands that are able to colloidally stabilize them in a polar solvent (methanol), maintaining about 60% of their initial QY. UV-Vis data suggested the presence of imidazoles in the ligand-exchanged samples; we confirmed by FTIR and VT-NMR that these histidine-derivative ligands bind to the QD surface via nucleophilic coordination of the imidazole anchoring group. However, coordination and colloidal stability are also promoted by the presence of a primary amine that contributes to charge balance at the QD surface. Ligand-exchanged QDs showed higher vibrational frequencies related to imidazole ring vibrations in FTIR and broadening of the imidazole ring proton at 6.89 ppm in the VT-NMR. Quantitative analysis of the ligand exchange demonstrates that up to 77% of the native oleate ligands have been removed from the QD surface. X-type exchange with Cl⁻ is the dominant process (68%) for removal of oleate from the QD surface while Z-type dissociation of the zinc oleate contributes the remainder. The ζ potential shifts to a positive value upon successful ligand exchange suggesting partial electrostatic stabilization in methanol. We expect that the library of small molecule imidazoles could serve as a model system to explore CdS and ZnS QD surfaces in aqueous environments relevant to bioimaging and other biomedical applications.

ASSOCIATED CONTENT

Supporting Information. Materials and detailed description of QD synthesis including hazards, Figures S1-S18 including additional FTIR and 1 H NMR characterization, ζ potential measurements, and SEM-EDAX analysis. This material is available free of charge via the Internet at http://pubs.acs.org.

AUTHOR INFORMATION

Corresponding Author

*Corresponding author: greytak@sc.edu.

Funding Sources

NSF CHE-MSN 2109064.

ACKNOWLEDGMENT

This work was supported by the US National Science Foundation under grant CHE-2109064.

REFERENCES

(1) Wu, X.; Liu, H.; Liu, J.; Haley, K. N.; Treadway, J. A.; Larson, J. P.; Ge, N.; Peale, F.; Bruchez, M. P. Immunofluorescent Labeling of Cancer Marker Her2 and Other Cellular Targets with Semiconductor Quantum Dots. *Nat Biotechnol* 2003, 21 (1), 41–46.

- (2) Alivisatos, P. The Use of Nanocrystals in Biological Detection. *Nature Biotechnology* **2004**, *22* (1), 47–52.
- (3) Erathodiyil, N.; Ying, J. Y. Functionalization of Inorganic Nanoparticles for Bioimaging Applications. *Acc Chem Res* **201**, 44 (10), 925–935.
- (4) Zhang, B.; Hu, R.; Wang, Y.; Yang, C.; Liu, X.; Yong, K.-T. Revisiting the Principles of Preparing Aqueous Quantum Dots for Biological Applications: The Effects of Surface Ligands on the Physicochemical Properties of Quantum Dots. *RSC Advances* 2014, 4 (27), 13805–13816.
- (5) Lemon, C. M.; Curtin, P. N.; Somers, R. C.; Greytak, A. B.; Lanning, R. M.; Jain, R. K.; Bawendi, M. G.; Nocera, D. G. Metabolic Tumor Profiling with PH, Oxygen, and Glucose Chemosensors on a Quantum Dot Scaffold. *Inorg. Chem.* **2014**, 53 (4), 1900–1915.
- (6) Giovanelli, E.; Muro, E.; Sitbon, G.; Hanafi, M.; Pons, T.; Dubertret, B.; Lequeux, N. Highly Enhanced Affinity of Multidentate versus Bidentate Zwitterionic Ligands for Long-Term Quantum Dot Bioimaging. *Langmuir* 2012, 28 (43), 15177–15184.
- (7) Tasso, M.; Giovanelli, E.; Zala, D.; Bouccara, S.; Fragola, A.; Hanafi, M.; Lenkei, Z.; Pons, T.; Lequeux, N. Sulfobetaine– Vinylimidazole Block Copolymers: A Robust Quantum Dot Surface Chemistry Expanding Bioimaging's Horizons. ACS Nano 2015, 9 (11), 11479–11489.
- (8) Bharthi, M. V.; Roy, N.; Moharana, P.; Ghosh, K.; Paira, P. Green Synthesis of Highly Luminescent Biotin Conjugated CdSe Quantum Dot for Bioimaging Application†. New J. Chem. 2020.
- (9) Eixenberger, J. E.; Anders, C. B.; Wada, K.; Reddy, K. M.; Brown, R. J.; Moreno-Ramirez, J.; Weltner, A. E.; Karthik, C.; Tenne, D. A.; Fologea, D.; Wingett, D. G. Defect Engineering of ZnO Nanoparticles for Bioimaging Applications. ACS Appl. Mater. Interfaces 2019, 11 (28), 24933–24944.
- (10) Dubertret, B.; Skourides, P.; Norris, D. J.; Noireaux, V.; Brivanlou, A. H.; Libchaber, A. In Vivo Imaging of Quantum Dots Encapsulated in Phospholipid Micelles. *Science* **2002**, 298 (5599), 1759–1762.
- (11) Leatherdale, C. A.; Woo, W.-K.; Mikulec, F. V.; Bawendi, M. G. On the Absorption Cross Section of CdSe Nanocrystal Quantum Dots. J. Phys. Chem. B 2002, 106 (31), 7619–7622.
- (12) Jasieniak, J.; Smith, L.; van Embden, J.; Mulvaney, P.; Califano, M. Re-Examination of the Size-Dependent Absorption Properties of CdSe Quantum Dots. *J. Phys. Chem. C* 2009, *11*3 (45), 19468–19474.
- (13) Smith, A. M.; Nie, S. Semiconductor Nanocrystals: Structure, Properties, and Band Gap Engineering. *Acc. Chem. Res.* **2010**, 43 (2), 190–200.
- (14) Liu, W.; Choi, H. S.; Zimmer, J. P.; Tanaka, E.; Frangioni, J. V.; Bawendi, M. Compact Cysteine-Coated CdSe(ZnCdS) Quantum Dots for in Vivo Applications. J. Am. Chem. Soc. 2007, 129 (47), 14530–14531.
- (15) Liu, W.; Howarth, M.; Greytak, A. B.; Zheng, Y.; Nocera, D. G.; Ting, A. Y.; Bawendi, M. G. Compact Biocompatible Quantum Dots Functionalized for Cellular Imaging. *J. Am. Chem. Soc.* **2008**, *130* (4), *1274–1284*.
- (16) Zimmer, J. P.; Kim, S.-W.; Ohnishi, S.; Tanaka, E.; Frangioni, J. V.; Bawendi, M. G. Size Series of Small Indium Arsenide-Zinc Selenide Core-Shell Nanocrystals and Their Application to in Vivo Imaging. J Am Chem Soc 2006, 128 (8), 2526–2527.
- (17) Aldana, J.; Wang, Y. A.; Peng, X. Photochemical Instability of CdSe Nanocrystals Coated by Hydrophilic Thiols. J. Am. Chem. Soc. 2001, 123 (36), 8844–8850.
- (18) Kessler, M. L.; Kelm, J. E.; Starr, H. E.; Cook, E. N.; Miller, J. D.; Rivera, N. A.; Hsu-Kim, H.; Dempsey, J. L. Unraveling Changes to PbS Nanocrystal Surfaces Induced by Thiols. *Chem. Mater.* 2022, 34 (4), 1710–1721.

- (19) Chen, P. E.; Anderson, N. C.; Norman, Z. M.; Owen, J. S. Tight Binding of Carboxylate, Phosphonate, and Carbamate Anions to Stoichiometric CdSe Nanocrystals. *J. Am. Chem. Soc.* **2017**, *139* (8), 3227–3236.
- (20) Ghani, S. F. A.; Wright, M.; Paramo, J. G.; Bottrill, M.; Green, M.; Long, N.; Thanou, M. Three Bisphosphonate Ligands Improve the Water Solubility of Quantum Dots. *Faraday Discuss.* 2014, 175, 153–169.
- (21) Weiss, E. A. Designing the Surfaces of Semiconductor Quantum Dots for Colloidal Photocatalysis. *ACS Energy Lett.* **2017**, 2 (5), 1005–1013.
- (22) Dennis, A. M.; Sotto, D. C.; Mei, B. C.; Medintz, I. L.; Mattoussi, H.; Bao, G. Surface Ligand Effects on Metal-Affinity Coordination to Quantum Dots: Implications for Nanoprobe Self-Assembly. *Bioconjug Chem* 2010, 21 (7), 1160–1170.
- (23) Hartley, C. L.; Dempsey, J. L. Revealing the Molecular Identity of Defect Sites on PbS Quantum Dot Surfaces with Redox-Active Chemical Probes. *Chem. Mater.* **2021**, *33* (7), 2655–2665.
- (24) Hartley, C. L.; Kessler, M. L.; Dones Lassalle, C. Y.; Camp, A. M.; Dempsey, J. L. Effects of Ligand Shell Composition on Surface Reduction in PbS Quantum Dots. *Chem. Mater.* 2021, 33 (22), 8612–8622.
- (25) Clapp, A. R.; Goldman, E. R.; Mattoussi, H. Capping of CdSe–ZnS Quantum Dots with DHLA and Subsequent Conjugation with Proteins. *Nature Protocols* **2006**, *1* (3), 1258–1266.
- (26) Vannoy, C. H.; Leblanc, R. M. Effects of DHLA-Capped CdSe/ZnS Quantum Dots on the Fibrillation of Human Serum Albumin. *J. Phys. Chem. B* **2010**, *114* (33), 10881–10888.
- (27) Reinhart, C. C.; Johansson, E. Colloidally Prepared 3-Mercaptopropionic Acid Capped Lead Sulfide Quantum Dots. *Chem. Mater.* 2015, 27 (21), 7313–7320.
- (28) Yildiz, I.; McCaughan, B.; Cruickshank, S. F.; Callan, J. F.; Raymo, F. M. Biocompatible CdSe–ZnS Core–Shell Quantum Dots Coated with Hydrophilic Polythiols. *Langmuir* **2009**, *25* (12), 7090–7096.
- (29) Turo, M. J.; Macdonald, J. E. Crystal-Bound vs Surface-Bound Thiols on Nanocrystals. ACS Nano 2014, 8 (10), 10205–10213.
- (30) Webber, D. H.; Brutchey, R. L. Ligand Exchange on Colloidal CdSe Nanocrystals Using Thermally Labile Tert-Butylthiol for Improved Photocurrent in Nanocrystal Films. *J. Am. Chem. Soc.* **2012**, *134* (2), 1085–1092.
- (31) Wuister, S. F.; de Mello Donegá, C.; Meijerink, A. Influence of Thiol Capping on the Exciton Luminescence and Decay Kinetics of CdTe and CdSe Quantum Dots. *J. Phys. Chem. B* **2004**, *108* (45), 17393–17397.
- (32) Johnson, C. M.; Pate, K. M.; Shen, Y.; Viswanath, A.; Tan, R.; Benicewicz, B. C.; Moss, M. A.; Greytak, A. B. A Methacrylate-Based Polymeric Imidazole Ligand Yields Quantum Dots with Low Cytotoxicity and Low Nonspecific Binding. *Journal of Colloid and Interface Science* 2015, 458, 310–314.
- (33) Dunlap, J. H.; Loszko, A. F.; Flake, R. A.; Huang, Y.; Benicewicz, B. C.; Greytak, A. B. Multiply-Binding Polymeric Imidazole Ligands: Influence of Molecular Weight and Monomer Sequence on Colloidal Quantum Dot Stability. *J. Phys. Chem. C* 2018, 122 (46), 26756–26763.
- (34) Zhang, P.; Liu, S.; Gao, D.; Hu, D.; Gong, P.; Sheng, Z.; Deng, J.; Ma, Y.; Cai, L. Click-Functionalized Compact Quantum Dots Protected by Multidentate-Imidazole Ligands: Conjugation-Ready Nanotags for Living-Virus Labeling and Imaging. J. Am. Chem. Soc. 2012, 134 (20), 8388–8391.
- (35) Grazon, C.; Chern, M.; Ward, K.; Lecommandoux, S.; Grinstaff, M. W.; Dennis, A. M. A Versatile and Accessible Polymer Coating for Functionalizable Zwitterionic Quantum Dots with High DNA Grafting Efficiency. *Chem. Commun.* **2019**, 55 (74), 11067–11070.

- (36) Wang, W.; van Niekerk, E. A.; Zhang, Y.; Du, L.; Ji, X.; Wang, S.; Groeniger, K.; Baker, J. D.; Raymo, F. M.; Mattoussi, H. Compact, "Clickable" Quantum Dots Photoligated with Multifunctional Zwitterionic Polymers for Immunofluorescence and In-Vivo Imaging. *Bioconjugate Chem.* 2020.
- (37) Wang, W.; Kapur, A.; Ji, X.; Safi, M.; Palui, G.; Palomo, V.; Dawson, P. E.; Mattoussi, H. Photoligation of an Amphiphilic Polymer with Mixed Coordination Provides Compact and Reactive Quantum Dots. *J. Am. Chem. Soc.* 2015, 137 (16), 5438–5451.
- (38) Liu, W.; Greytak, A. B.; Lee, J.; Wong, C. R.; Park, J.; Marshall, L. F.; Jiang, W.; Curtin, P. N.; Ting, A. Y.; Nocera, D. G.; Fukumura, D.; Jain, R. K.; Bawendi, M. G. Compact Biocompatible Quantum Dots via RAFT-Mediated Synthesis of Imidazole-Based Random Copolymer Ligand. *J. Am. Chem. Soc.* 2010, 132 (2), 472–483.
- (39) Viswanath, A.; Shen, Y.; Green, A. N.; Tan, R.; Greytak, A. B.; Benicewicz, B. C. Copolymerization and Synthesis of Multiply Binding Histamine Ligands for the Robust Functionalization of Quantum Dots. *Macromolecules* **2014**, *47* (23), 8137–8144.
- (40) Viswanath, A.; Paudel, P.; Kittikhunnatham, P.; Green, A. N.; Greytak, A. B.; Benicewicz, B. C. Synthesis of Random Terpolymers Bearing Multidentate Imidazole Units and Their Use in Functionalization of Cadmium Sulfide Nanowires. *Polym. Chem.* **2015**, *6* (39), 7036–7044.
- (41) Takeuchi, H.; Omogo, B.; Heyes, C. D. Are Bidentate Ligands Really Better than Monodentate Ligands For Nanoparticles? *Nano Lett* **2013**, *13* (10), 4746–4752.
- (42) Anderson, N. C.; Chen, P. E.; Buckley, A. K.; De Roo, J.; Owen, J. S. Stereoelectronic Effects on the Binding of Neutral Lewis Bases to CdSe Nanocrystals. *J. Am. Chem. Soc.* **2018**, *140* (23), 7199–7205.
- (43) Shen, Y.; Gee, M. Y.; Tan, R.; Pellechia, P. J.; Greytak, A. B. Purification of Quantum Dots by Gel Permeation Chromatography and the Effect of Excess Ligands on Shell Growth and Ligand Exchange. *Chem. Mater.* 2013, 25 (14), 2838–2848.
- (44) Gee, M. Y.; Shen, Y.; Greytak, A. B. Isothermal Titration Calorimetry Resolves Sequential Ligand Exchange and Association Reactions in Treatment of Oleate-Capped CdSe Quantum Dots with Alkylphosphonic Acid. J. Phys. Chem. C 2020.
- (45) Greytak, A. B.; Tan, R.; Roberts, S. K. Prospects for Rational Control of Nanocrystal Shape Through Successive Ionic Layer Adsorption and Reaction (SILAR) and Related Approaches. In *Anisotropic and Shape-Selective Nanomaterials: Structure-Property Relationships*; Hunyadi Murph, S. E., Larsen, G. K., Coopersmith, K. J., Eds.; Nanostructure Science and Technology; Springer International Publishing: Cham, 2017; pp 169–232.
- (46) Lindroos, S.; Leskelä, M. Successive Ionic Layer Adsorption and Reaction (SILAR) and Related Sequential Solution-Phase Deposition Techniques. In *Solution Processing of Inorganic Materials*; Mitzi, D. B., Ed.; John Wiley & Sons, Inc., 2008; pp 239–282.
- (47) Tan, R.; Blom, D. A.; Ma, S.; Greytak, A. B. Probing Surface Saturation Conditions in Alternating Layer Growth of CdSe/CdS Core/Shell Quantum Dots. *Chem. Mater.* **2013**, 25 (18), 3724–3736.
- (48) Brouwer, A. M. Standards for Photoluminescence Quantum Yield Measurements in Solution (IUPAC Technical Report). *Pure and Applied Chemistry* **2011**, 83 (12), 2213–2228.
- (49) Morrison, C.; Sun, H.; Yao, Y.; Loomis, R. A.; Buhro, W. E. Methods for the ICP-OES Analysis of Semiconductor Materials. *Chem. Mater.* **2020**, 32 (5), 1760–1768.
- (50) Rezaei, M. T.; Keypour, H.; Bayat, M.; Soltani, E.; Jamshidi, M.; Gable, R. W. Synthesis of a Tertiary Amine by Direct Re-

- ductive Amination of a Carbonyl Compound to Form a Scorpionate Ligand; Formation of Mn (II), Zn (II) and Cd (II) Complexes, DFT Calculations and, Molecular Docking Studies. *Journal of Molecular Structure* **2021**, *1224*, 129119.
- (51) Young, A. G.; Al-Salim, N.; Green, D. P.; McQuillan, A. J. Attenuated Total Reflection Infrared Studies of Oleate and Trioctylphosphine Oxide Ligand Adsorption and Exchange Reactions on CdS Quantum Dot Films. *Langmuir* 2008, 24 (8), 3841–3849.
- (52) Balakrishnan, G.; Jarzecki, A. A.; Wu, Q.; Kozlowski, P. M.; Wang, D.; Spiro, T. G. Mode Recognition in UV Resonance Raman Spectra of Imidazole: Histidine Monitoring in Proteins. *J. Phys. Chem. B* **2012**, *116* (31), 9387–9395.
- (53) Zhao, X.; Shen, Y.; A. Adogla, E.; Viswanath, A.; Tan, R.; C. Benicewicz, B.; B. Greytak, A.; Lin, Y.; Wang, Q. Surface Labeling of Enveloped Virus with Polymeric Imidazole Ligand-Capped Quantum Dots via the Metabolic Incorporation of Phospholipids into Host Cells. *Journal of Materials Chemistry B* 2016, 4 (14), 2421–2427.
- (54) Jana, N. R.; Patra, P. K.; Saha, A.; Basiruddin, S.; Pradhan, N. Imidazole Based Biocompatible Polymer Coating in Deriving

- <25 Nm Functional Nanoparticle Probe for Cellular Imaging and Detection. *J. Phys. Chem. C* 2009, *11*3 (52), 21484–21492.
- (55) Wang, W.; Ji, X.; Kapur, A.; Zhang, C.; Mattoussi, H. A Multifunctional Polymer Combining the Imidazole and Zwitterion Motifs as a Biocompatible Compact Coating for Quantum Dots. J. Am. Chem. Soc. 2015, 137 (44), 14158–14172.
- (56) Greytak, A. B.; Allen, P. M.; Liu, W.; Zhao, J.; Young, E. R.; Popović, Z.; Walker, B. J.; Nocera, D. G.; Bawendi, M. G. Alternating Layer Addition Approach to CdSe/CdS Core/Shell Quantum Dots with near-Unity Quantum Yield and High on-Time Fractions. *Chem. Sci.* 2012, 3 (6), 2028–2034.
- (57) Beecher, A. N.; Yang, X.; Palmer, J. H.; LaGrassa, A. L.; Juhas, P.; Billinge, S. J. L.; Owen, J. S. Atomic Structures and Gram Scale Synthesis of Three Tetrahedral Quantum Dots. *J. Am. Chem. Soc.* **2014**, *136* (30), 10645–10653.
- (58) Anderson, N. C.; Owen, J. S. Soluble, Chloride-Terminated CdSe Nanocrystals: Ligand Exchange Monitored by 1H and 31P NMR Spectroscopy. *Chem. Mater.* **2013**, *25* (1), 69–76.

Synopsis: A small-molecule imidazole ligand system is demonstrated that can bring CdSe/ZnS core/shell quantum dots into methanol solution. Coordination is via the imidazole lone pair with charge balance via simultaneous coordination of excess metal equivalents on the nanocrystal by chloride.

